A storm surge inundation model of the northern Bay of Bengal using publicly available data

Matt Lewis,[a,b]* Paul Bates,[b] Kevin Horsburgh,[a] Jeff Neal[b] and Guy Schumann[b]

[a]*National Oceanography Centre, Liverpool, UK*
[b]*School of Geographical Sciences, University of Bristol, UK*

*Correspondence to: M. Lewis, National Oceanography Centre, Joseph Proudman Building,6 Brownlow Street, Liverpool L3 5DA, UK. E-mail: matwis@noc.ac.uk

A computationally inexpensive inundation model has been developed from freely available data sources for the northern Bay of Bengal region to estimate flood risk from storm surges. This is the first time Shuttle Radar Topography Mission (SRTM) terrain data have been used in a dynamic coastal inundation model. To reduce SRTM noise, and the impact of vegetation artefacts on the ground elevation, the SRTM data were up-scaled from their native 90 m resolution to 900 m. A sub-grid routine allowed estuary channels with widths less than this resolution to be simulated efficiently, and allowed six major river flows to be represented. The inundation model was forced with an IIT-D model hindcast of the 2007 cyclone *Sidr* flood event, using parameters from two cyclone databases (IBTrACs and UNISYS). Validation showed inundation prediction accuracy with a root mean squared error (RMSE) on predicted water level of ∼ 2 m, which was of the same order of magnitude as the forcing water-level uncertainties. Therefore, SRTM and other publicly available data can be useful for coastal flood risk management in data-poor regions, although the associated uncertainty needs to be expressed to end users. Better SRTM processing techniques may improve inundation model performance, and future work should also seek to improve storm tide uncertainties in this region. Copyright © 2012 Royal Meteorological Society

Key Words: SRTM; IIT-D; cyclone *Sidr*; storm surge; inundation

Received 8 March 2012; Revised 3 August 2012; Accepted 19 August 2012; Published online in Wiley Online Library 15 October 2012

Citation: Lewis M, Bates P, Horsburgh KJ, Neal J, Schumann G. 2013. A storm surge inundation model of the northern Bay of Bengal using publicly available data. *Q. J. R. Meteorol. Soc.* **139**: 358–369. DOI:10.1002/qj.2040

1. Introduction

Tropical cyclones have led to some of the most notable coastal flooding disasters in recent history. The change in atmospheric pressure and extreme wind stress result in a storm surge that temporarily raises the total water level, producing a storm tide which can flood vast areas of land. In Bangladesh, cyclone-generated storm tides have resulted in the deaths of over 700 000 people since 1960 (Chowdhury and Karim, 1996). Flood risk in Bangladesh is high because geomorphic and bathymetric effects enhance the storm surge height in this densely populated, low-lying, deltaic region (Murty *et al.*, 1986; Dube *et al.*, 1997). One such example of a recent cyclone-induced coastal flooding event was the 2007 cyclone *Sidr* event. This was a category 4 storm that made landfall at approximately 1700 UTC on 15 November 2007 on the Bangladesh coastline (89.8°E), resulting in a 5.8 m surge (Dube *et al.*, 2009), leaving 3406 people dead and causing damage nearly totalling US$1.7 billion (Dube *et al.*, 2009; Paul, 2009). The relatively low number of deaths was considered the result of the cyclone early warning system, cyclone shelters and landfall location (Paul, 2009). Obvious challenges to be tackled to further reduce future fatalities include: (1) considering climate change implications (e.g. Karim and Mimura, 2008); (2) estimating coastal flood risk to guide cyclone shelter construction (Chowdhury and

Karim, 1996; Chowdhury *et al.*, 1998); and (3) correctly predicting inundation extent in real time, as part of an early warning system (including forecast uncertainties).

Good reviews of numerical storm surge modelling in the Bay of Bengal can be found in Murty *et al.* (1986) and Dube *et al.* (1997), and these explain the development of depth-averaged (2D) hydrodynamic models that solve the shallow-water equations. Many of these hydrodynamic models include wetting and drying, allowing a moveable coastal boundary that can represent storm surge generation and inundation simultaneously (e.g. Flather, 1994; Madsen and Jakobsen, 2004;). These storm surge models are forced with an idealised cyclone model of wind and pressure fields (Jelenianski and Taylor, 1973; Holland, 1980), using predicted or observed cyclone data (track, central pressure and radius of maximum winds).

Although full hydrodynamic models can simulate the physics of flood inundation well, this approach can be computationally expensive at a resolution useful to flood hazard/risk assessment (Bates *et al.*, 2005; Hunter *et al.*, 2007). Full shallow-water equation models may be overspecified for many gradually varying flooding problems (Neal *et al.*, 2012) and increasing model resolution may be a better way to improve predictive accuracy than including a more detailed physical process representation. Model resolution is particularly important for inundation modelling because channels need to be correctly resolved to allow storm tide penetration upstream and inland. Inclusion of river flow also allows the simulation of backwater effects (Ali, 1995; Agnihotri *et al.*, 2006). The nesting of numerical hydrodynamic models can improve computational efficiency at resolution scales useful to flood risk managers (Madsen and Jakobsen, 2004); however, nationwide inundation models with a grid size of the order of kilometres are currently considered to be of high resolution in the region (Debsarma, 2009). One recent solution has been the use of an unstructured grid finite-element approach (e.g. Rao *et al.*, 2010); however this approach is still computationally expensive, especially if major flood hazard uncertainty sources are to be included in the analysis.

There are many sources of uncertainty in predicting inundation extent, perhaps best split into two areas: (1) intra-model uncertainties affecting the simulation of the flood wave inland, such as model resolution, or the choice of bed roughness values; and (2) extra-model uncertainties, such as the errors within the Digital Elevation Model (DEM) or the forcing water-level boundary condition (e.g. peak storm tide height) for the model. In the UK, uncertainties of coastal flood hazard and risk modelling were shown to be high, and the inclusion of major sources of uncertainty was found to be necessary for robust flood risk prediction (Lewis *et al.*, 2011). It can be assumed that uncertainties would be greater in data-poor regions such as Bangladesh; therefore, a computationally efficient approach may be required so a probabilistic framework can be implemented to evaluate the effect of these uncertainties (Aronica *et al.*, 2002; Purvis *et al.*, 2008).

One compromise to allow simulation of inundation at a regional scale could be the use of a hydrodynamic model which solves a simplified form of the shallow-water equations (e.g. Syme and Apelt, 1990; Bates *et al.*, 2005). The latest formulation of one such model (LISFLOOD-FP) is computationally efficient (Bates *et al.*, 2010), yet includes sufficient shallow-water physics to simulate gradually varied sub-critical flows accurately where high-quality terrain and forcing data are available (Neal *et al.*, 2012). The LISFLOOD-FP model solves an local inertial approximation to the full shallow-water equations using a finite-difference technique and is described in detail elsewhere (Bates *et al.*, 2010).

The accuracy of such inundation models is, to a great extent, limited by data quality. Higher-resolution topographic data (e.g. LiDAR) necessary to simulate flood wave propagation accurately is costly and not available for the Bay of Bengal. The suitability of publicly available data for inundation models therefore needs to be assessed for the management of coastal inundation risks. The main aim of this article is to develop a LISFLOOD-FP inundation model of the northern Bay of Bengal based on only freely available data sources, and test the model against maximum water-level observations taken during the 2007 *Sidr* event. This event was chosen because, perhaps uniquely, observations of the flooding have been published (ITJSCE, 2008; IWM, 2009; Paul, 2009).

Uncertainty in simulated storm surge magnitude arises from meteorological uncertainty (Madsen and Jakobsen, 2004). Therefore, cyclone *Sidr* observations from two cyclone databases will be used to force the storm surge model: UNISYS (http://weather.unisys.com/hurricane/n_indian/index.html; 2010) and IBTrACs (http://www.ncdc.noaa.gov/oa/ibtracs; 2010). The storm surge model used in this work has been developed by the Indian Institute of Technology Delhi (IIT-D), and is the same model used for operational storm surge forecasting in the region (Dube *et al.*, 1997; Debsarma, 2009), a task for which it has shown accuracy (Dube *et al.*, 2009). The IIT-D model is a fully nonlinear, depth-averaged, hydrodynamic storm surge model, forced by the Jelenianski and Taylor (1973) cyclone wind field model. Therefore, the predicted water levels at the coast from the IIT-D model were used as the coastal boundary condition to force the LISFLOOD-FP model of the flooding inland.

Topographic data used to generate the DEM for the LISFLOOD-FP inundation model were taken from the freely available (http://srtm.csi.cgiar.org; 2010) 3 arc second resolution Shuttle Radar Topography Mission (SRTM) dataset (Jarvis *et al.*, 2004, 2008). SRTM data have been successfully used in fluvial flood models (e.g. Valeriano *et al.*, 2006; Sanders, 2007; Wilson *et al.*, 2007), and to delineate coastal flood risk zones (Demirkesen *et al.*, 2007); however, the suitability of SRTM data for use in dynamic coastal inundation models is unknown due to resolution accuracy, and vegetation effects within the SRTM data (Ludwigm and Scheider, 2006; Wilson *et al.*, 2007).

2. Methodology

2.1. *DEM generation methodology*

The reported absolute global vertical accuracy of SRTM data is ± 16 m at the 90% confidence level (Jarvis *et al.*, 2008); however, the absolute accuracy of SRTM data is much higher in low-slope areas like the delta region of Bangladesh (Jarvis *et al.*, 2004; Rodriguez *et al.*, 2006; Reuter *et al.*, 2007). Instead, the SRTM random vertical noise (∼ 6 m at the native 90 m SRTM resolution) and impact of vegetation artefacts on absolute accuracy are likely to be much larger issues than SRTM absolute accuracy, and are considered in more detail

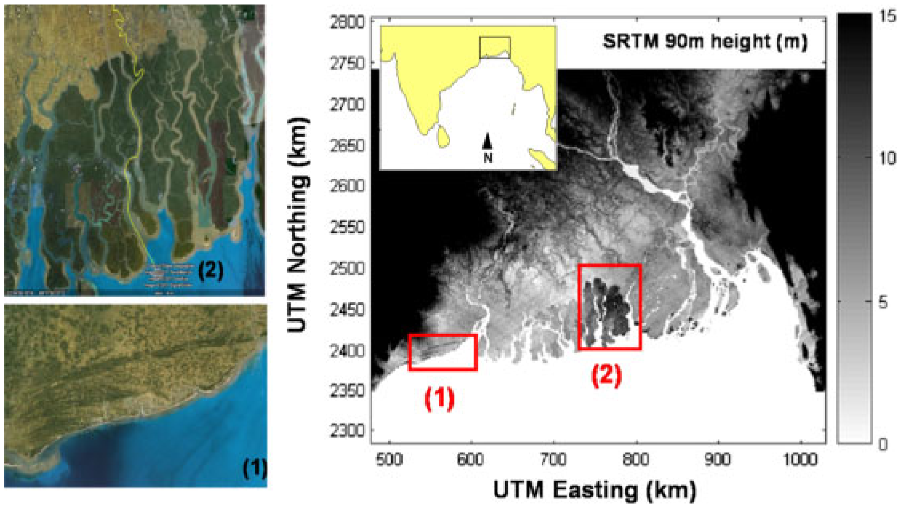

Figure 1. Two examples (boxes (1) and (2)) of vegetation features within the Shuttle Radar Topography Mission (SRTM) data over the northern Bay of Bengal (right), compared with images from Google earth (left; http://earth.google.co.uk/). This figure is available in colour online at wileyonlinelibrary.com/journal/qj

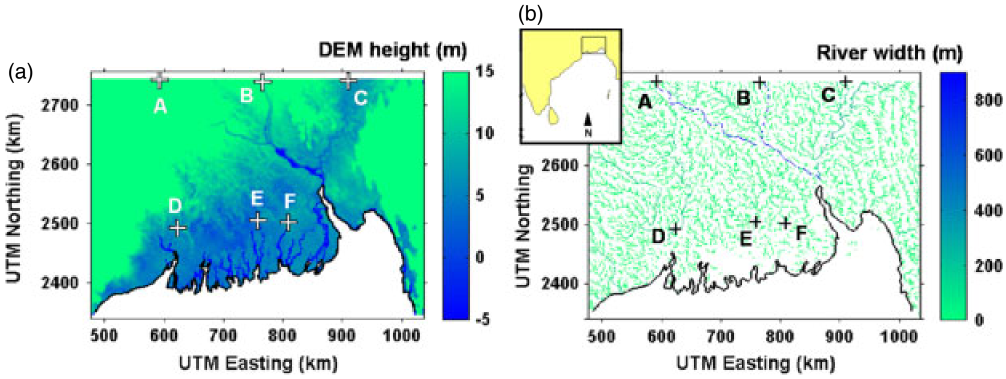

Figure 2. (a) The Digital Elevation Model (DEM) of the northern Bay of Bengal from processed and 900 m averaged SRTM data, and (b) the assumed river widths for the same region, taken from publicly available data (HydroSHEDS) used in the LISFLOOD-FP inundation model to simulate river channels with length-scales less than DEM resolution (sub-grid channel routine) using hydraulic geometry theory. The forcing coastal boundary is shown as a black line, and point source locations of six major rivers included in the model are also shown: Ganges (A), Brahmaputra (B), Meghna (C), Damodar (D), Pussur (E), and Baleswar (F). This figure is available in colour online at wileyonlinelibrary.com/journal/qj

below. It is well known that vegetation artefacts are contained within the SRTM data (e.g. Ludwigm and Scheider, 2006; Valeriano *et al.*, 2006) as the X- and C-band radars used for the SRTM mission do not penetrate vegetation canopies fully. Indeed, suspect vegetation features found within the SRTM data for the northern Bay of Bengal are compared to Google earth images (http://www.earth.google.co.uk) in Figure 1. These vegetation features of Figure 1 also correlate with the freely available (http://www.landcover.org; 2011) 1 km land-use map from the 1981–1994 Advanced Very High Resolution Radiometer (AVHRR) of Hansen *et al.*, (1998; 2000). Unfortunately, the technique of assigning an SRTM height correction for each vegetation class in the land-use data (Wilson *et al.*, 2007; Getirana *et al.*, 2009) was not possible in this study because of high SRTM within-class variance. Indeed, no statistical correlation was found between the AVHRR land-use image and SRTM data within the assumed flood plain (heights less than 20 m) using a 900 m averaging window. This is presumably due to the high SRTM data spatial variance (approximately 6 m in the raw 90 m SRTM data), as reported by many authors (e.g. Rodriquez *et al.*, 2006; Valeriano *et al.*, 2006), and the variability of vegetation species (and thus vegetation height) within a land-use zone. Using the AVHRR land-use image (http://www.landcover.org; 2011) and Google earth images, vegetation-affected regions in the SRTM data were removed and a nearest-neighbour interpolation technique used to replace SRTM heights in the vegetation-affected regions to generate a 90 m UTM projected Digital Terrain Model (DTM).

The spatial noise of SRTM, and thus artificial roughness of the 90 m DTM, is assumed to reduce linearly in proportion to $1/\sqrt{n}$, where n is the number of pixels averaged (Rodriguez *et al.*, 2006; Wilson *et al.*, 2007). Using a smoothing and averaging window, a 900 m DEM was generated (Figure 2), as at this resolution the signal to noise ratio (SNR) was reduced to an acceptable level within the flood plain (45% of data had SNR>2:1 for STRM heights less than 10 m). DEM cells that correlated to water within Google earth images or AVHRR water-body regions were removed as SRTM data cannot penetrate water. The IIT-D storm surge model bathymetry was interpolated to the DEM and missing bathymetry data within estuaries were estimated during LISFLOOD-FP model calibration (section 2.2). Hydraulic geometry theory, which relates river depth and width to river discharge and catchment area (Leopold and Maddock, 1953) and which has been successfully used for rivers in the Bay of Bengal region (Islam and Karim, 2005), was used to aid this process. River channel depths were estimated using hydraulic geometry theory, and simulated within the LISFLOOD-FP model using a sub-grid channel routine (Neal *et al.*, 2012), which allows rivers with widths less than the DEM resolution to be simulated within LISFLOOD-FP. A river channel width raster (Figure 2) was created from the freely available HydroSHEDS stream network raster file (http://hydrosheds.cr.usgs.gov/hydro.php; 2011). Indeed, unpublished preliminary work indicated that the 900 m DEM and river width sub-grid routine could simulate the theoretical maximum combined (Ganges, Brahmaputra and Meghna) flow rate of 74 000 m^3 s^{-1} without flooding (Rasid and Paul, 1987; Islam and Sado, 2000), suggesting that river depths and bank heights were successfully estimated.

Six rivers were included in the LISFLOOD-FP model as point sources flux rates (locations are shown A to F in Figure 2). Actual discharge rates for the *Sidr* event are unknown, therefore published observations during the cyclone season (April–May, October–December) were used and the following river flow rates assumed: (a) Ganges, 3000 m^3 s^{-1} (Khalil, 1990); (b) Brahmaputra, 6000 m^3 s^{-1} (Khalil, 1990); (c) Meghna, 850 m^3 s^{-1} (Khalil, 1990); (d) Damodar, 200 m^3s^{-1} (http://www.grdc.sr.unh.edu/html/Polygons/P2854050.html; 2010); (e) Pussur, 300 m^3s^{-1} (Nobi and Gupta, 1997); (f) Baleswar, 1500 m^3s^{-1} (Nobi and Gupta, 1997).

2.2. *LISFLOOD-FP calibration methodology*

Hydraulic geometry theory is used to represent river channels in the DEM, but cannot be used to estimate estuarine bathymetry because different processes are involved. Considering the importance of river channels as a mechanism of coastal flooding in Bangladesh, any assumed estuary depth will need to be calibrated. Dredging activities from the port authorities in some estuaries does keep the bathymetry constant; for example the Pussur River channel is dredged to approximately 6 m (http://www.starpathgroup.net/port.html; 2011). However, bathymetry of other estuaries in the northern Bay of Bengal region is complex due to annual and inter-annual variability of sedimentation rates (Ali *et al.*, 2007). Observations by Ali *et al.* (2007) showed the Meghna estuary depth to be between approximately 3 m and 6 m (with a 15 m deep navigation channel). Therefore, the missing bathymetry data within the DEM were assumed to be within the range 0 to 9 m during model calibration.

Bed roughness (represented here using the Manning coefficient) controls the progression of the flood wave within the LISFLOOD-FP model, and can be defined according to land use (e.g. Chow, 1959) but is typically adjusted during calibration. To understand the uncertainty associated with the estuary depth assumption, the Manning values were assumed to be spatially constant and to vary between 0.018 and 0.28 during estuary depth calibration. The Manning roughness range of 0.018 and 0.28 reflects typical values used to represent bare earth and mangrove regions respectively (Chow, 1959; Furukawaa *et al.*, 1997; Musleh and Cruise, 2006). As a range of Manning roughness values were used in the estuary depth calibration, the results from such a sensitivity test allowed a spatially varying Manning roughness map to be made for the LISFLOOD-FP validation to the 2007 *Sidr* event using the freely available (http://www.landcover.org) 1981–1994 AVHRR 1 km land-use map (Hansen *et al.*, 1998, 2000), discussed in section 3.2.

Karim and Mimura (2008) forced a 1D hydrodynamic model (Chowdhury and Karim, 1996) with a 9.2 m idealized storm tide to give estimated water-level heights along the length of the Pussur Estuary (shown as point E, approximately at 760 km easting in Figure 2). The LISFLOOD-FP model was forced with this 9.2 m idealized storm tide along the length of the open coastal boundary (Figure 2), for a simulation time of 30 h, which took less than an hour to complete on a desktop PC. The results of this 9.2 m idealised storm tide test allowed the sensitivity of flood extent to be investigated for bathymetry errors and Manning roughness coefficient uncertainties to be investigated.

2.3. *LISFLOOD-FP 2007 cyclone Sidr validation methodology*

The storm surge of the 2007 cyclone *Sidr* event was simulated with the IIT-D model. The atmospheric variables of central pressure (dp, assuming ambient of 1013 hPa), cyclone track (latitude ψ, and longitude), maximum wind speed ($V_{\max}$ m s^{-1}) and radius of maximum winds ($R_{\max}$ km), used to force the Jelenianski and Taylor (1973) idealized cyclone wind and pressure model, were taken from two freely available cyclone databases (surge scenarios A and B respectively): Unisys (http://weather.unisys.com/hurricane/n_indian/index.html; 2010) and IBTrACs (http://www.ncdc.noaa.gov/oa/ibtracs; 2010). $R_{\max}$ was not available from either cyclone database, and so was estimated using the Willoughby *et al.* (2006) equation from the IBTrACs analysis:

$$R_{\max} = 46.4 \exp(-0.0155\, V_{\max} + 0.0169\psi). \qquad (1)$$

The Unisys database had no central pressure values available for the *Sidr* event, so values of central pressure were taken from Dube *et al.* (2009).

The peak simulated surges using the available data from UNISYS and IBTrACs (surge scenarios A and B) were 4.37 m and 6.22 m respectively, as shown in Figure 3. The peak surge heights of scenario A and B were interpolated to the open coastal boundary of the LISFLOOD-FP model (BC) and averaged into piecewise constant sections, as shown in Figure 3. The storm surge time series was assumed to be represented by a sinusoid (duration 12 h) with the peak surge occurring at 1630 UTC (0.5 h before *Sidr* landfall). Tidal height and phase were estimated from the UK Admiralty tide tables for the region (Table 1) and interpolated to the LISFLOOD-FP boundary (Figure 3). The resultant surge and tide time series (assuming a period of 12.42 h) were combined to produce a spatially varying storm tide time series. Examples of these time series are shown in Figure 4 (for storm surge scenario B), and were used to force the LISFLOOD-FP model. The 2007 *Sidr* peak storm tide (total water level excluding waves) was calculated to be 5.00 m and 6.74 m at the coast for the storm surge scenarios A and B respectively. Wave set-up and tide–surge interaction (Johns *et al.*, 1985) were not included in the IIT-D simulations, and therefore not all water-level uncertainty was propagated into the LISFLOOD-FP model, although the storm surge is significantly larger than the tidal amplitude, and thus tide–surge interaction is likely to be second-order.

The resultant inundation simulated by LISFLOOD-FP, for storm surge scenarios A and B, was validated using

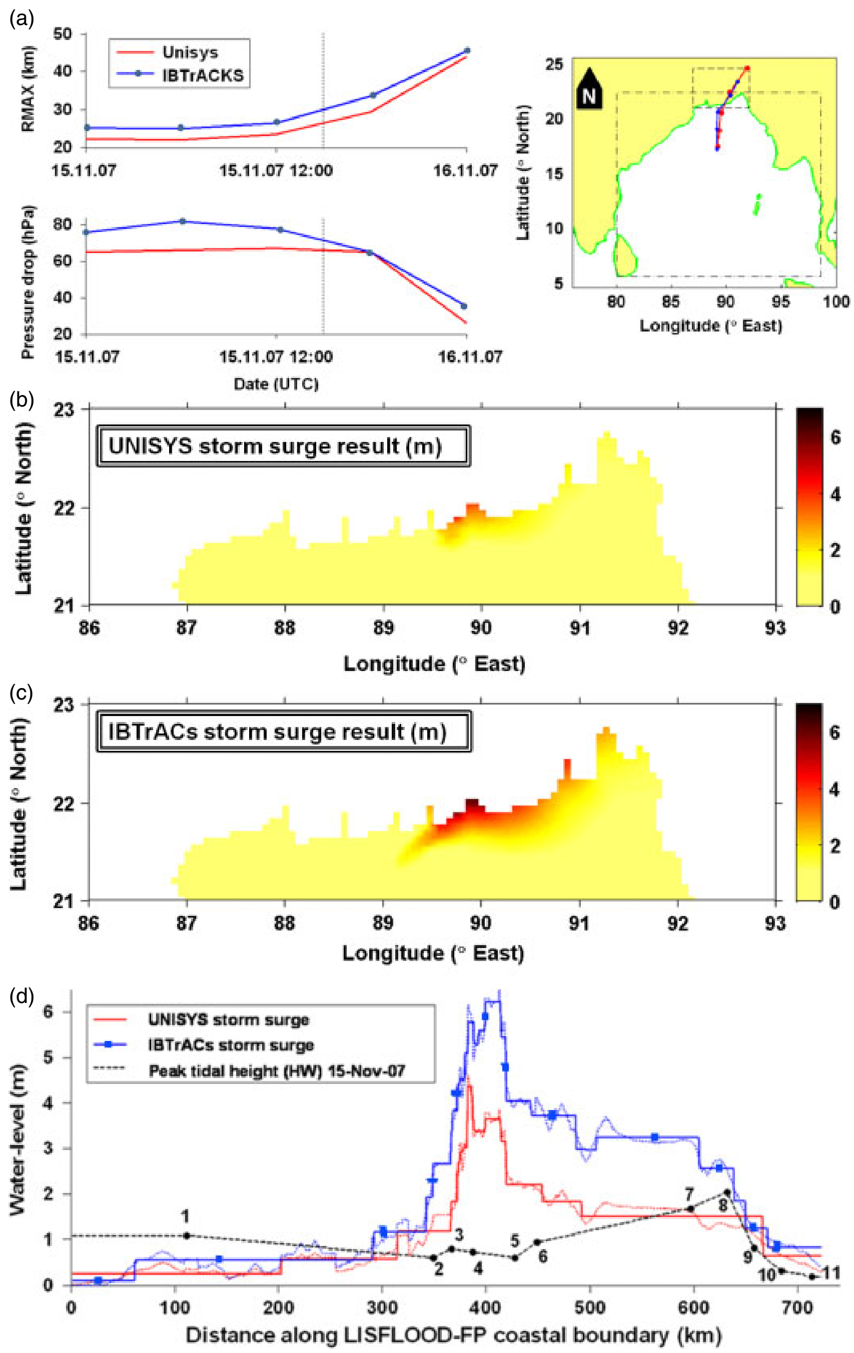

Figure 3. (a) Data from two cyclone databases, UNISYS and IBTrACS, for the Bay of Bengal 2007 cyclone *Sidr* event, and (b, c) the peak storm surge heights from the IIT-D simulations. (d) shows the peak storm surge and tidal heights interpolated to the LISFLOOD-FP coastal boundary. This figure is available in colour online at wileyonlinelibrary.com/journal/qj

Table 1. The 2007 Admiralty published astronomical peak tide height (HW) and times for three standard ports (*) and eight secondary ports in the northern Bay of Bengal during the 2007 cyclone *Sidr* flood.

Port name	ID	Location (°N, °E)		15 Nov 2007 HW (m wrt to msl)	Time (UTC) of 15 Nov 2007 HW
Sagar Roads*	1	21.65	88.05	1.10	1733
Pussur River*	2	21.80	89.47	0.60	1908
Jefford Point	3	21.73	89.55	0.80	1843
Tiger Point	4	21.85	89.83	0.73	1908
Dhulasar	5	21.85	90.25	0.60	1933
Rabnabad Channel	6	22.07	90.37	0.94	2008
Hatia Bar	7	22.48	90.95	1.69	2338
Sandwip Island	8	22.50	91.42	2.05	2238
Chittagong*	9	22.33	91.83	0.82	2238
Kutubdia Island	10	21.87	91.83	0.31	2034
Cox's Bazar	11	21.43	91.98	0.19	1923

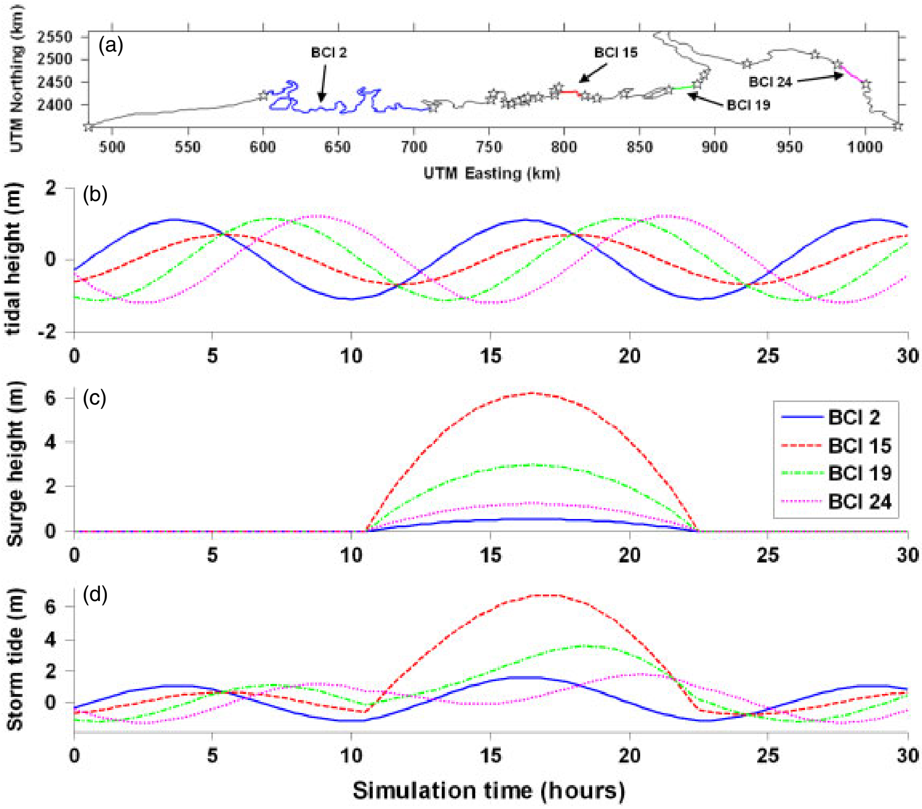

Figure 4. The assumed components (b) tide and (c) storm surge of (d) the total water-level time series (storm tide) for storm surge scenario B for four LISFLOOD-FP coastal boundary sections (BCI 2, 15, 19 and 24; locations shown in (a)), used to force the inundation model to simulate the inundation of the 2007 cyclone *Sidr* event. This figure is available in colour online at wileyonlinelibrary.com/journal/qj

Table 2. Details of thirteen water-level observations of the 2007 *Sidr* flood, collated from a number of sources and used to validate the LISFLOOD-FP inundation model of the northern Bay of Bengal.

ID	Location(°N, °E)		Flood height (m) wrt msl	Water depth (m) wrt ground	Reference
1	22.30	89.85	5		IWM(2009); Paul (2009)
2	22.45	89.60	3		IWM (2009)
3	22.31	89.85	1.97		ITJSCE (2008)
4	22.31	89.86		1.98	ITJSCE (2008)
5	22.23	89.83	6.47		ITJSCE (2008)
6	22.70	90.31		1.8–2.1	IWM (2009)
7	22.82	90.33		1.5–1.8	IWM (2009)
8	22.55	90.35		1.5–1.8	IWM (2009)
9	22.37	90.32		2.1–2.7	IWM (2009)
10	22.48	90.07		1.5–2.4	IWM (2009)
11	22.57	89.98		0.5–0.9	IWM (2009)
12	22.47	89.85		0.9–2.4	IWM (2009)
13	22.37	90.16		0.5–0.9	IWM (2009)

Flood height observations are measured with respect to (wrt) the river level, which we assume to be mean sea level (msl), whilst water depth observations are measured as heights above the ground (wrt ground).

observations of flood water levels from several publications (ITJSCE, 2008; IWM, 2009; Paul, 2009). To reduce observed water-level uncertainty, flood observations were included only if the precise location was available and the variability of raw SRTM height data within the DEM cell coincident with the observed data point was below an acceptable level (SNR>2:1). The thirteen inundation observations that remain after this quality control are shown in Table 2. As shown in Figure 5, there is still a degree of simulated flood level uncertanty due to observational uncertainty and the variance of SRTM heights (within each corresponding DEM cell). Observation locations IDs 1, 2, 3 and 5 correspond to estuary channel locations within the DEM grid (we assume a DEM value of −6 m for these locations), matching observations. However, this resulted in no SRTM data being available for DEM uncertainty assessments at ID 3, whilst only limited data were available at IDs 1,2 and 5. Further uncertainty may be present from errors of water-level estimation during *Sidr* flood surveys, however it was not possible to include this within our analysis.

LISFLOOD-FP performance in simulating the flooded area using storm surge scenarios A and B was also evaluated using data from an ENVISAT Advanced Synthetic Aperture Radar (ASAR) image acquired four days after the event on 19 November 2007 (© ESA). Flooding on the ASAR image was extracted using a simple but very widely used

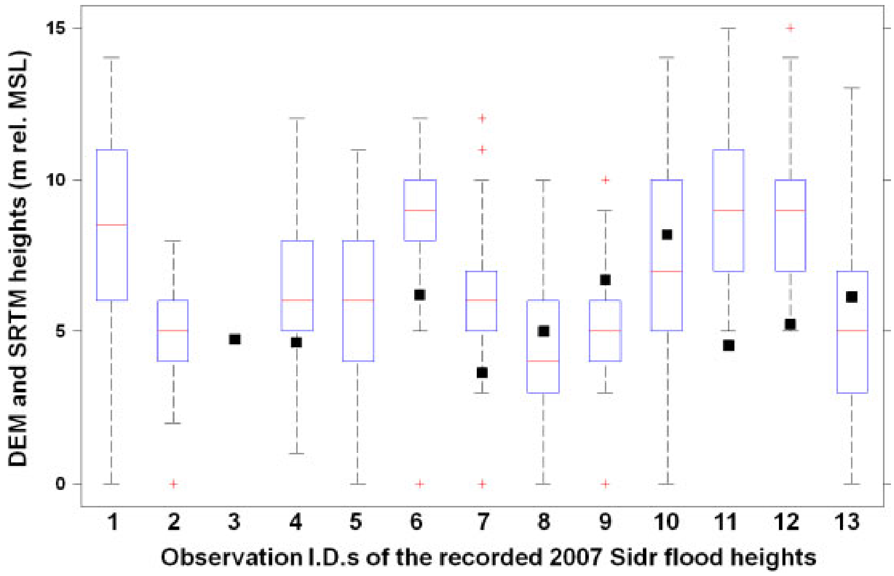

Figure 5. The variability of raw SRTM data used to calculate the DEM height (black squares) for thirteen 2007 cyclone *Sidr* flood observations. Crosses indicate SRTM outliers, whilst the absence of DEM heights (solid squares) at ID locations 1, 2, and 5 indicate DEM estuary channel locations (assumed -6 m). This figure is available in colour online at wileyonlinelibrary.com/journal/qj

image histogram threshold method (Otsu, 1979). This fully automated method thresholds an image into black and white areas (i.e. dry and wet pixels) by applying a criterion measure to evaluate the between-class variance of a threshold at a given greyscale level computed from a normalized image grey level histogram. Here, we extended this technique further to account for uncertainty in the process by using a range of a large number of possible greyscale level thresholds and aggregating the binary map results to a single final map that shows for each pixel the probability of it being wet based on the outcomes of the many algorithm realisations. In the flood map shown in Figure 6, a pixel with a value of 1 was classified as wet every time the algorithm was run and a pixel with a value of 0 was never wet, with different frequencies of wet classifications represented by values between 0 and 1. The freely available 19 November MODIS flood map (http://www.dartmouth.edu/~floods/images/2 007 219Bang.jpg) was used as a 'control' to determine the wet state probability of Figure 6 with which to evaluate model performance. Pixels with a probability of being wet greater than 0.85 (excluding permanent water bodies) in the SAR image (Figure 6) were assumed to represent the observed flood extent.

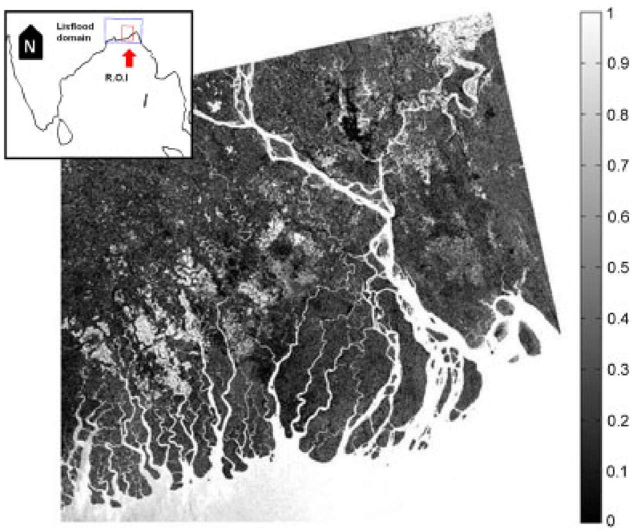

Figure 6. Synthetic Aperture Radar (SAR) map of 19 November 2007, showing wet state probability (0 to 1) for each pixel (see text for more explanation) for the region of interest (ROI) of the 2007 cyclone *Sidr* flood event. This figure is available in colour online at wileyonlinelibrary.com/journal/qj

3. Results

3.1. LISFLOOD-FP calibration results

The simulated inundation extent sensitivity to Manning roughness choice and estuarine bathymetry uncertainty was investigated using the Karim and Mimura (2008) idealized 9.2 m storm tide. Manning roughness had the greatest effect on simulated flood extent whilst bathymetry uncertainty (within estuaries) had a much greater effect than DEM uncertainty (based on the standard deviation of the SRTM 900 m average ground elevation). The modification of the storm tide as it propagates upstream can be seen in Figure 7, which shows the peak storm tide along the Pussur River channel (Point E of Figure 2), and a storm tide time series at various points along the estuary length (A to E of Figure 7). The storm tide is modified considerably if the channel bathymetry is less than 6 m. Nevertheless, based on our assumed bathymetry range (0–9 m), the Manning's roughness value choice appears to have a greater effect on storm tide propagation than bathymetry uncertainty. Indeed, for large Manning coefficient values the water-level time series is modified even at the mouth of the estuary (0 km in Figure 7). The effect of three Manning roughness scenarios is summarized in Figure 8, and compares the Karim and Mimura (2008) result to the range of peak storm tide heights along the Pussur River for an assumed bathymetry range between 0 and 9 m (hence the overplotting of ranges between $n = 0.1$ and $n = 0.28$ in Figure 8).

The Manning roughness values shown in Figure 8 are within the typical range (Chow, 1959; Furukawaa *et al.*, 1997; Bates *et al.*, 2005; Musleh and Cruise, 2006) of

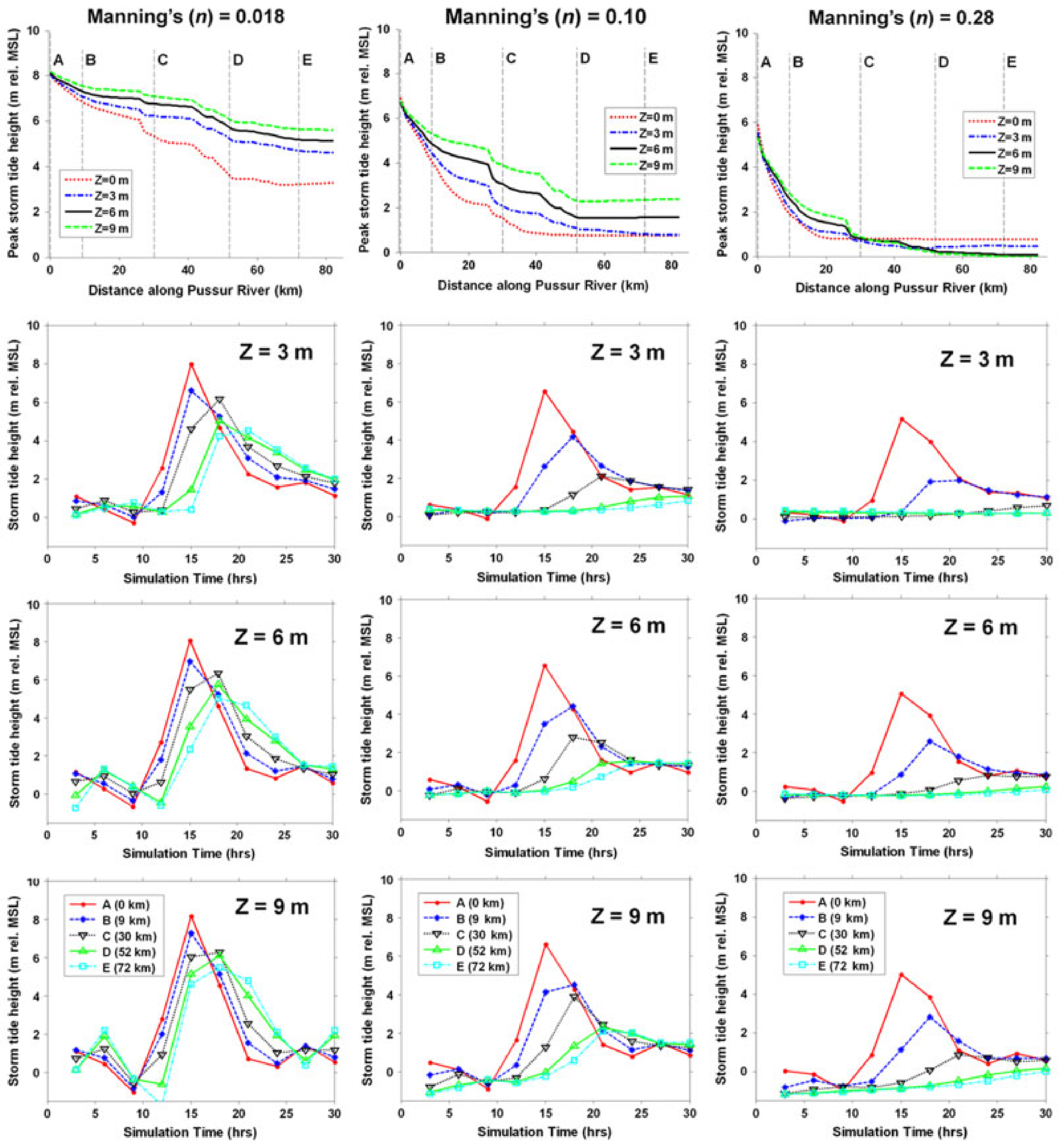

Figure 7. The LISFLOOD-FP simulated propagation of a 9.2 m storm tide upstream in the Pussur River, Bangladesh, for three Manning roughness (n) and estuary depth (z) scenarios with the modification of the water-level time series at five locations (A to E) for distances 0 (river mouth), 9, 30, 52 and 72 km. This figure is available in colour online at wileyonlinelibrary.com/journal/qj

roughness coefficients for bare earth (0.018) to mangroves (0.2–0.28). The roughness range is perhaps unrealistically wide, however it shows how Manning roughness can control flood wave propagation more than bathymetry choice. For the LISFLOOD-FP simulation of cyclone *Sidr*, the estuary depth was assumed to be 6 m (−6 m wrt SRTM), and, using the AVHRR land-use image (http://www.landcover.org), roughness values of 0.02 (water regions), 0.05 (grassland and low vegetation regions), 0.1 (shrubland regions) and 0.2 (mangrove regions) were chosen to create a spatially varying Manning roughness map based on land use, as shown in Figure 9.

3.2. *2007 cyclone Sidr LISFLOOD_FP validation results*

The SRTM derived DEM (900 m resolution), assuming 6 m bathymetry in estuaries and the Manning roughness coefficient spatial distribution shown in Figure 9, was used for the LISFLOOD-FP simulation of the 2007 cyclone *Sidr* flood event. An initial condition, based on a one month tide only (no storm surge) and river simulation, was used as a 'hot start' before forcing the LISFLOOD-FP model with storm surge scenarios A and B. A simulation of 30 h took less than 1 h to complete on a desktop PC, for a domain size of 561.6 km × 396.9 km (275 184 cells, or ∼223 000 km^2), with the latest formulation of the LISFLOOD-FP code (Bates

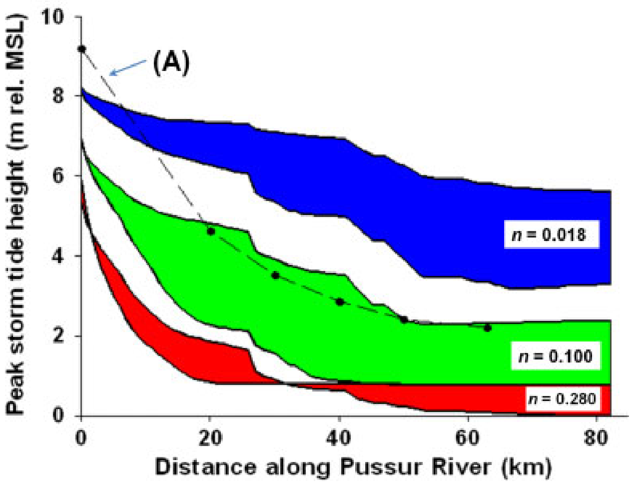

Figure 8. The peak storm tide height along the length of the Pussur River, Bangladesh (0 km at river mouth), with assumed sensitivity of bathymetry uncertainty (0 to 9 m) expressed as the shaded area for three Manning roughness scenarios ($n = 0.018, 0.1, 0.28$), compared to the hydrodynamic model (A) of Karim and Mimura (2008). This figure is available in colour online at wileyonlinelibrary.com/journal/qj

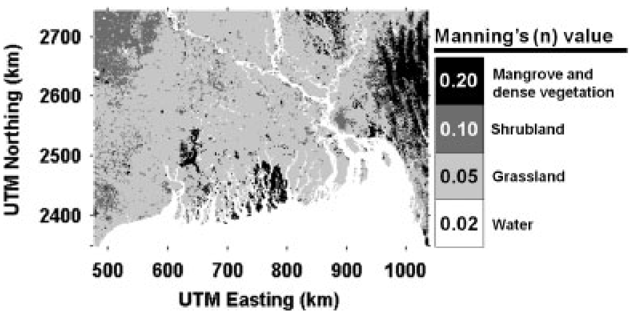

Figure 9. Assumed Manning roughness coefficient values (n) for the northern Bay of Bengal used for inundation model validation of the 2007 cyclone *Sidr* flood event.

et al., 2010). The flooded area simulated by LISFLOOD-FP, calculated as the area above that flooded in a tide-only run (the initial 'hot-start' file), was 8379 km^2 and 10 035 km^2 for storm surge scenarios A and B respectively, as shown in Table 3. Using a combined image dataset consisting of a permanent water mask and SAR pixels of a wet state probability >0.85 (section 2.3), we applied a modified version of the reliability diagram method as outlined in Di Baldassarre *et al.* (2009). For regions of SAR probabilities >0.85, the proportion of simulated wet cells in a perfect model would match the observed proportions (assuming no observation error). In the region of interest (Figure 6) the agreement between the observed probabilities and predicted proportion of wet pixels/cells of peak flood extent, excluding permanently wet areas, was 41% and 43% for the storm surge scenarios A and B respectively. The agreement between observed and LISFLOOD-FP simulated flood extent could be improved as the majority of rivers within the region of interest were not simulated within the LISFLOOD-FP model and there are likely to be inaccuracies because of terrain data errors.

Thirteen maximum water-level observations (Table 2) were used to estimate inundation model performance using the Root Mean Squared Error (RMSE) between observed and simulated water-level heights (Table 3). An overall RMSE of inundation model performance was calculated as

Table 3. The performance of the LISFLOOD-FP inundation model in simulating thirteen observations of flooding during the 2007 cyclone *Sidr* flood event, forced with two storm surge scenarios (from UNISYS and IBTrACS databases).

	UNISYS (A)	IBTrACS (B)
Simulated flood area (km^2)	8379	10035
RMSE (m) of flood heights (4 observations)	2.77	2.14
RMSE (m) of flood depths (9 observations)	1.78	1.78
Overall RMSE (m) from 13 observations	2.13	1.89
Flood agreement (wet cell and ASAR observed)	41%	43%

2.13 m and 1.89 m for the storm surge scenarios A and B respectively, which is similar to the LISFLOOD-FP boundary forcing uncertainty. The difference between the peak storm surge simulated by IIT-D using data available from UNISYS (scenario A; 4.37 m) and IBTrACs (scenario B; 6.22 m) data was 1.85 m. The LISFLOOD-FP boundary forcing uncertainty is likely to be much greater than this 1.85 m storm surge difference between the two scenarios because of uncertainties introduced when adding the assumed tidal time series to generate the LISFLOOD-FP coastal forcing water-level condition.

Uncertainty of the 13 flood observations due to DEM resolution (Figure 5) was accounted for by projecting the SRTM varibility as one standard deviation (sd) either side of the simulated inundation water level. If this DEM uncertainty is included, only two of the validation locations are not flooded by the LISFLOOD-FP model (86% success in both storm surge scenarios), and eight of the observed flood levels are within the LISFLOOD-FP simulated inundation height range (red line of Figure 10). The LISFLOOD-FP model was run assuming a uniform minimum (0.018) and maximum (0.28) Manning roughness coefficient which, although unlikely, gives the maximum range of inundation water level the model can simulate with calibration. The inundation water-level range (shown in Figure 10 as circles) indicated that only six locations (46% success) can be flooded with a different Manning roughness spatial formulation. Therefore, the inability of the LISFLOOD-FP inundation model to flood all of the 13 validation locations is mainly due to DEM and boundary forcing (water-level) errors, rather than a calibration issue.

4. Discussion

Using a DEM built from freely available data sources, a regional-scale inundation model of the northern Bay of Bengal has been developed using the latest formulation of LISFLOOD-FP (Bates *et al.*, 2010; Neal *et al.* 2012). This type of modelling approach is computationally much cheaper than full hydrodynamic models (Bates *et al.*, 2010), and therefore could be used to investigate (e.g. Lewis *et al.*, 2011) and quantify (e.g. Aronica *et al.*, 2002; Purvis *et al.*, 2008) the DEM and water-level uncertainties highlighted in this article.

SRTM data has been used previously to delineate coastal flood risk zones (Demirkisen *et al.*, 2007), or within fluvial flood models (e.g. Valeriano *et al.*, 2006; Sanders, 2007; Wilson *et al.*, 2007); however, this is the first time the SRTM data have been used for a dynamic coastal inundation model. The well-known (and problematic) vegetation effects typically found within SRTM data (e.g.

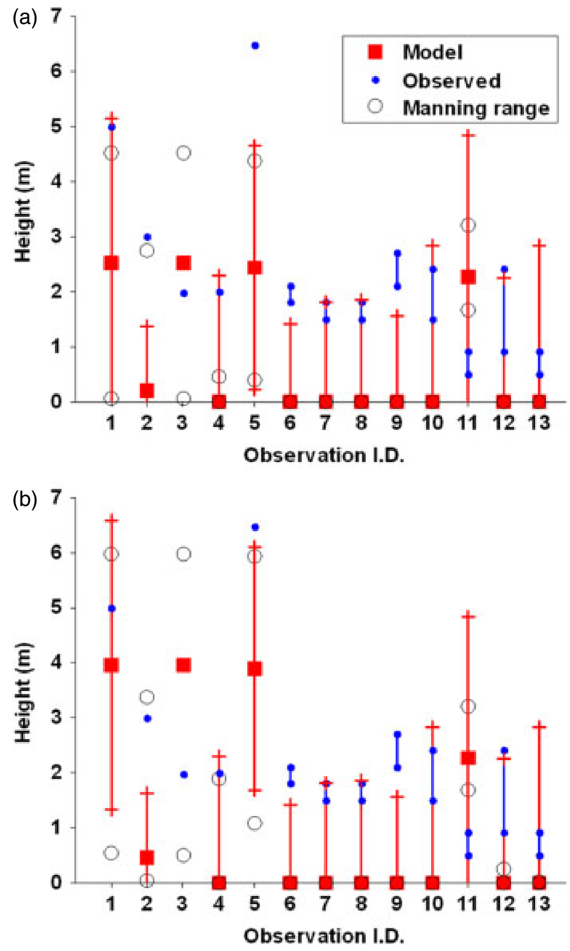

Figure 10. Validation of the northern Bay of Bengal LISFLOOD-FP model simulated flood depths (solid squares) against thirteen observations (closed circles) of flooding during the 2007 cyclone *Sidr* event for two storm surge scenarios based on data from cyclone databases UNISYS (A) and IBTrACs (B). Topographic error within the inundation model, due to DEM resolution, is included as one standard deviation of SRTM variance (crosses joined by solid lines), and the effect of the Manning roughness coefficient choice (high, 0.28, and low, 0.018) is represented by open circles. This figure is available in colour online at wileyonlinelibrary.com/journal/qj

Valeriano *et al.*, 2006) were also present in the Bay of Bengal region. Previous vegetation processing techniques (e.g. Valeriano *et al.* 2006; Getirana *et al.*, 2009) could not be performed because of a high degree of noise and poor correlation statistics. Therefore, vegetation-affected regions of the SRTM data were removed using a freely available (http://www.landcover.org) AVHRR land-use map (Hansen *et al.*, 1998; 2000). The remaining SRTM data were interpolated and averaged to a 900 m DEM grid to reduce random noise to an acceptable level (~ 1 m). Coastal defence embankments are present in Bangladesh and India (ITJSCE, 2008), but were not included because of a lack of published information on defence crest elevations. The presence of coastal defences is assumed to have little effect on the *Sidr* inundation extent because of the widespread erosion and overtopping observed (ITJSCE, 2008; Paul, 2009).

The correct simulation of storm surge propagation upstream in rivers and estuaries, along with simulation of the backwater effect of river flows, is important for coastal inundation modelling in low-lying deltas. River channels with widths less than the DEM resolution could be simulated within LISFLOOD-FP using a sub-grid channel routine (Neal *et al.*, 2012). The inundation model showed accuracy at predicting the inundation of the 2007 cyclone *Sidr* flood, as the difference between simulated and observed *Sidr* flood water levels (RMSE of 2.13 m and 1.89 m for storm surge scenarios A and B) was attributed to DEM error and errors in the water-level data used to force LISFLOOD-FP. Indeed, model performance could be improved with the inclusion of observed flood-level uncertainties, and better data on actual river flows (only assumed flow rates of six major rivers were included). Resolution is obviously important for accurate inundation modelling and LISFLOOD-FP has shown skill in data-rich regions (e.g. Bates *et al.*, 2005). Therefore, better vegetation removal and processing of SRTM data would lead to production of a finer-scale, more accurate, DEM and an improvement in model performance if correct forcing water-level information were known.

Storm surge uncertainty is known to be high in the Bay of Bengal (e.g. Madsen and Jakobsen, 2004), and such boundary condition uncertainty was expressed within inundation model validation with storm surge scenarios from two cyclone databases (IBTrACs and UNISYS). The UNISYS data-forced peak storm surge was 4.89 m and the peak storm tide was estimated to be 5.00 m, which differs from the 5.8 m calculated by Dube *et al.* (2009) because of different approaches in estimating the tidal component of the storm tide, and the inclusion of storm development (time-varying R_{max}) within this study. The difference between storm tide scenarios A and B was 1.74 m (storm surge difference of 1.85 m, with a 30 min time difference in peak surge); hence forcing water-level uncertainty was found to be of the same order of magnitude as the inundation model error (RMSE). Further water-level effects that contribute to the total storm tide height at the coast, such as tide–surge interaction (Johns *et al.*, 1985), air–sea drag coefficient choice (e.g. Moon *et al.*, 2007), and wave set-up (which can add 0.5 m to total water levels at the coast; Jain *et al.*, 2010) were not included in forcing the LISFLOOD-FP inundation model. Additional water-level uncertainty was introduced from the interpolation of tidal data, and assumptions made to generate the spatially varying water-level time series used to force the LISFLOOD-FP coastal boundary.

5. Conclusion

A computationally inexpensive regional-scale inundation model has been developed from freely available data sources for the northern Bay of Bengal and tested against the 2007 cyclone *Sidr* event. Uncertainties from freely available data sources (such as SRTM) are high; however data availability is very limited in the northern Bay of Bengal. Therefore, SRTM and other publicly available data can be of use to flood risk management in data-poor regions if the uncertainty is correctly communicated to end users. Finer-scale DEMs, from better SRTM processing techniques, would allow more accurate simulation of inundation; however, the LISFLOOD-FP error (RMSE) at this site was found to be of the same order of magnitude as forcing water-level uncertainty for a hindcast event. Considering the uncertainties inherent in future storm tide conditions (e.g. extreme water-level estimates), it appears that boundary forcing uncertainty may be much greater than SRTM-generated DEM uncertainty within the inundation model. Therefore, future storm surge flood risk models in data-poor regions can be made from publicly available data, but future work should investigate the magnitude of uncertainty in current and future flood risk inundation studies in the Bay of Bengal. One application for the LISFLOOD-FP inundation model developed within this article could be as part of a cyclone early warning flood forecast; alternatively it could be used to improve future coastal flood risk understanding in the northern Bay of Bengal region because uncertainties could be included in a probabilistic framework (e.g. Aronica *et al.*, 2002; Purvis *et al.*, 2008) and communicated to policy makers.

Acknowledgements

Matt Lewis is a PhD student funded by a UK Engineering and Physical Science Research Council (EPSRC) studentship as part of the Flood Risk Management Research Consortium (FRMRC). The authors also would like to thank Professor Shishir Dube from the Indian Institute of Technology (Delhi) for the use of the IIT-D storm surge model, and Dr Tomohiro Yasuda for the quality-checked IBTrACs version2 dataset.

References

Agnihotri N, Chittibabu P, Jain I, Sinha PC, Rao AD, Dube SK. 2006. A bay–river coupled model for storm surge prediction along the Andhra coast of India. *Natural Hazards* **39**: 83–101.

Ali A. 1995. Numerical investigation into the retardation of flood water outflow through the Meghna river in Bangladesh due to SW monsoon wind. *Estuarine Coastal Shelf Sci.* **41**: 689–704.

Ali A, Mynett AE, Azam MH. 2007. Sediment dynamics in the Meghna Estuary Bangladesh: A model study. *J. Waterway Port Coastal Ocean Eng.* **133**: 255–263.

Aronica G, Bates PD, Horritt MS. 2002. Assessing the uncertainty in distributed model predictions using observed binary pattern information within GLUE. *Hydrol. Proc.* **16**: 2001–2016.

Bates PD, Dawson RJ, Hall JW, Horritt MS, Nicholls RJ, Wicks J, Hassan MAAMH. 2005. Simplified two-dimensional numerical modelling of coastal flooding and example applications. *Coastal Eng.* **52**: 793–810.

Bates PD, Horritt MS, Fewtrell TJ. 2010. A simple inertial formulation of the shallow-water equations for efficient two-dimensional flood inundation modelling. *J. Hydrol.* **387**: 33–45.

Chow VT. 1959. *Open Channel Hydraulics*. McGraw-Hill: New York.

Chowdhury JU, Karim MF. 1996. A risk-based zoning of storm surge prone area of the Ganges Tidal Plain. *J. Civil Eng.* (Institution of Engineering, Bangladesh) **24**: 221–233.

Chowdhury JU, Watkins DW, Rahman R, Karim F. 1998. Models for cyclone shelter planning in Bangladesh. *Water Internat.* **23**: 155–163.

Debsarma SK. 2009. Simulations of storm surges in the Bay of Bengal. *Marine Geodesy* **32**: 178–198.

Demirkesen AC, Evrendilek F, Berberoglu S, Kilic S. 2007. Coastal flood risk analysis using Landsat-7 ETM+ imagery and SRTM DEM: A case study of Izmir, Turkey. *Environ. Monitoring Assess.* **131**: 293–300.

Di Baldassarre G, Schumann G, Bates PD. 2009. A technique for the calibration of hydraulic models using uncertain satellite observations of flood extent. *J. Hydrol.* **367**: 276–282.

Dube SK, Rao AD, Sinha PC, Murty TS, Bahulayan N. 1997. Storm surge in the Bay of Bengal and Arabian Sea: the problem and its prediction. *Mausam* **48**: 283–304.

Dube SK, Jain I, Rao AD, Murty TS. 2009. Storm surge modelling for the Bay of Bengal and Arabian Sea. *Natural Hazards* **51**: 3–27.

Flather RA. 1994. A storm surge prediction model for the northern Bay of Bengal with application to the cyclone disaster in April 1991. *J. Phys. Oceanogr.* **24**: 172–190.

Furukawaa K, Wolanskic E, Mueller H. 1997. Currents and sediment transport in mangrove forests. *Estuarine Coastal Shelf Sci.* **44**: 301–310.

Getirana ACV, Bonnet MP, Martinez JM. 2009. Evaluating parameter effects in a DEM 'burning' process based on land cover data. *Hydrol. Proc.* **23**: 2316–2325.

Hansen MC, DeFries RS, Townshend JRG, Sohlberg R. 1998. 'UMD Global Land Cover Classification, 1 Kilometer 1.0'. Department of Geography: University of Maryland, College Park, Maryland, 1981–1994.

Hansen MC, DeFries RS, Townshend JRG, Sohlberg R. 2000. Global land cover classification at 1 km spatial resolution using a classification tree approach. *Internat. J. Remote Sensing* **21**: 1331–1364.

Holland GJ. 1980. An analytical model of the wind and pressure profiles in hurricanes. *Mon. Weather Rev.* **108**: 1212–1218.

Hunter NM, Bates PD, Horritt MS, Wilson MD. 2007. Simple spatially distributed models for predicting flood inundation: a review. *Geomorphol.* **90**: 208–225.

Islam M, Sado K. 2000. Flood hazard assessment in Bangladesh using NOAA AVHRR data with geographical information system. *Hydrol. Proc.* **14**: 605–620.

Islam T, Karim R. 2005. Predicting downstream hydraulic geometry of the Gorai river. *J. Civil Eng.* **33**: 55–63.

ITJSCE. 2008. 'Investigation report on the storm surge disaster by cyclone *Sidr* in November 2007 in Bangladesh'. (Transient translation, 2008). Investigation Team of Japan Society of Civil Engineering. http://www.jsce.or.jp/report/46/files/Bangladesh_Investigation.pdf

IWM. 2009. 'Use of existing data on available digital elevation models to prepare useable tsunami and storm surge inundation risk maps for the entire coastal region. Final report Vol. I: Tsunami and strom surge inundation of the coastal area of Bangladesh'. Institute of Water Modelling: Bangladesh. http://www.cdmprm.org.bd/eq/17.pdf

Jain I, Rao AD, Ramesh KJ. 2010. Vulnerability asessment at village level due to tide, surges and wave set-up. *Marine Geodesy* **33**: 245–260.

Jarvis A, Rubiano J, Nelson A, Farrow A, Mulligan M. 2004. 'Practical use of SRTM data in the tropics: Comparisons with digital elevation models generated from cartographic data'. Working Document no. 198. International Centre for Tropical Agriculture (CIAT): 32.

Jarvis A, Reuter HI, Nelson A, Guevara E. 2008. 'Hole-filled seamless SRTM data v4'. International Centre for Tropical Agriculture (CIAT). http://srtm.csi.cgiar.org

Jelenianski CP, Taylor AD. 1973. 'A preliminary view of storm surges before and after storm modification'. Technical Memo. WMPO-3, 23–33. Environmental Research Laboratories, National Oceanic and Atmospheric Administration: Washington DC.

Johns B, Rao AD, Dube SK, Sinha PC. 1985. Numerical modelling of tide–surge interaction in the Bay of Bengal. *Phil. Trans. R. Soc. London* **A313**: 507–535.

Karim MF, Mimura N. 2008. Impacts of climate change and sea-level rise on cyclonic storm surge floods in Bangladesh. *Global Environ. Change* **18**: 490–500.

Khalil GMD. 1990. Floods in Bangladesh: A question of disciplining the rivers. *Natural Hazards* **3**: 379–401.

Leopold LB, Maddock TJ. 1953. 'Hydraulic geometry of stream channels and some physiographic implications'. Professional paper 252. US Geological Survey: Reston, Virginia.

Lewis M, Horsburgh K, Bates P, Smith R. 2011. Quantifying the uncertainty in future coastal flood risk estimates for the UK. *J. Coastal Res.* **27**: 870–881.

Ludwigm R, Schneider P. 2006. Validation of digital elevation models from SRTM X-SAR for applications in hydrologic modelling. *ISPRS J. Photogramm.Remote Sensing* **60**: 339–358.

Madsen H, Jakobsen F. 2004. Cyclone induced storm surge and flood forecasting in the northern Bay of Bengal. *Coastal Eng.* **51**: 277–296.

Moon IJ, Ginis I, Hara T, Thomas B. 2007. A physics-based parameterization of air–sea momentum flux at high wind speeds and its impact on hurricane intensity predictions. *Mon. Weather Rev.* **135**: 2869–2878.

Murty TS, Flather RA, Henry RF. 1986. The storm surge problem in the Bay of Bengal. *Prog. Oceanogr.* **16**: 195–233.

Musleh FA, Cruise JF. 2006. Functional relationships of resistance in wide flood plains with rigid unsubmerged vegetation. *J. Hydraul. Eng.* **132**: 162–171.

Neal J, Villanueva I, Wright N, Willis T, Fewtrell T, Bates P. 2012. How much physical complexity is needed to model flood inundation? *Hydrol. Proc.* **26**: 2264–2282.

Nobi N, Gupta AD. 1997. Simulation of regional flow and salinity intrusion in an integrated stream–aquifer system in coastal region: Southwest region of Bangladesh. *Ground Water* **35**: 786–796.

Otsu N. 1979. A threshold selection method from gray-level histograms. *IEEE Trans. Syst. Man. Cybernet.* **9**: 62–66.

Paul BK. 2009. Why relatively fewer people died? The case of Bangladesh's cyclone *Sidr*. *Natural Hazards* **50**: 289–304.

Purvis MJ, Bates PD, Hayes CM. 2008. A probabilistic methodology to future coastal flood risk due to sea-level rise. *Coastal Eng.* **55**: 1062–1073.

Rao AD, Jain I, Venkatesan R. 2010. Estimation of extreme water levels due to cyclonic storms: A case study for Kalpakkam coast. *Internat. J. Ocean Climate Syst.* **1**: 1–14.

Rasid H, Paul BK. 1987. Flood problem in Bangladesh: Is there an indigenous solution? *Environ. Manage.* **11**: 155–173.

Reuter HI, Nelson A, Jarvis A. 2007. An evaluation of void filling interpolation methods for SRTM data. *Internat. J. Geograph. Inform. Sci.* **21**: 983–1008.

Rodriguez E, Morris CS, Belz JE. 2006. A global assessment of the SRTM performance. *Photogramm. Eng. Remote Sensing* **72**: 249–260.

Sanders BF. 2007. Evaluation of online DEMs for flood inundation modelling. *Adv.Water Resources* **30**: 1831–1843.

Syme WJ, Apelt CJ. 1990. 'Linked two-dimensional/one-dimensional flow modelling using the shallow-water equations'. In *Proceedings of the Conference on Hydraulics in Civil Engineering*, Barton, ACT, Australia. Institution of Engineers: Australia, 28–32.

Valeriano MM, Kuplich TM, Storino M, Amaral BD, Mendes JN, Lima DJ. 2006. Modelling small watersheds in Brazilian Amazonia with shuttle radar topographic mission 90 m data. *Computers Geosci.* **32**: 1169–1181.

Willoughby HE, Darling RWR, Rahn ME. 2006. Parametric representation of the primary hurricane vortex. Part 2: A new family of sectionally continuous profiles. *Mon. Weather Rev.* **134**: 1102–1120.

Wilson MD, Bates PD, Alsdorf D, Forsberg B, Horritt MS, Melack J, Frappart F, Famiglietti J. 2007. Modelling large-scale inundation of Amazonian seasonally flooded wetlands. *Geophys. Res. Lett.* **34**: L15404, DOI: 10.1029/2007GL030156.

